Surface functionalization of cotton cellulose with glycidyl methacrylate and its application for the adsorption of aromatic pollutants from wastewaters

Elena Vismara [a,*], Lucio Melone [a], Giuseppe Gastaldi [a], Cesare Cosentino [b], Giangiacomo Torri [b]

[a] Dipartimento di Chimica, Ingegneria Chimica e Materiali "G. Natta" del Politecnico di Milano, Via Mancinelli 7, 20131 Milano, Italy
[b] Istituto di Ricerche Chimiche e Biomediche "G. Ronzoni", Via G. Colombo 81, 20133 Milano, Italy

ARTICLE INFO

ABSTRACT

Cellulose material **C1** was prepared by grafting of glycidyl methacrylate (GMA) in the presence of Fenton-type reagent. This one-pot procedure provided **C1** with glycidyl isobutyrate branches. Glycidyl epoxide ring opening with water turned **C1**–**C2** material branched with glycerol isobutyrate. So, **C1** surface bears hydrophobic branches ending with the glycidyl group, while **C2** surface presents hydrophilic branches ending with the glycerol group. The adsorption of aromatic polluting substances like phenol (Ph), 4-nitrophenol (pNPh), 2,4-dinitrophenol (dNPh), 2,4,6-trinitrophenol (picric acid, tNPh) and 2-naphtol (BN) from their water solutions was tested with **C1**, **C2** and with the untreated cellulose material **C0**. Phenol adsorption did not occur. All the other aromatic molecules were removed in different amount both by **C1** and **C2**. **C1** and **C2** showed different affinities towards nitrophenols and 2-naphtol. While **C1** was much more effective for removing the hydrophobic 2-naphtol, **C2** had higher adsorption capacity towards the hydrophilic nitrophenols, in agreement with their branches polarity, respectively.

© 2009 Elsevier B.V. All rights reserved.

1. Introduction

In recent years many efforts have been done in the field of the removal of aromatic pollutants from wastewater. Nowadays there is a wide choice of techniques having both qualities and deficiencies not only from a technical point of view, but also from an economic one.

Some of these strategies are directed toward the degradation of organic contaminants by chemical oxidation [1,2], electrolysis [3] and biodegradation [4] while others are based on physico-chemical separations like solvent extraction [5], membrane separation [6,7] and adsorption [8–10]. Adsorption seems to have a wide field of application due to many factors: simplicity of design, ease of operations, and wide choice of adsorbent materials, effectiveness and possibility of regeneration of the adsorbents.

Many attempts have also been pursued toward the use of cheap and effective adsorbents, in particular natural materials, bio-sorbents and waste materials from agriculture and industry. An extensive review of the application of non-conventional adsorbents for the removal of dyes from water has been recently published by Crini [11]. Following this trend, cellulose-based adsorbents could be good candidates for wastewater treatment. Cellulose, one of the most abundant, renewable and cheap natural polymers, can be manufactured in several forms like yarns, woven and non woven fabrics, sheets, giving to the users a wide range of choice for several process conditions. By itself, cellulose is not able to adsorb aromatic pollutants and, as far as we know, there are no references about simple and cheap chemical or physical modifications, suitable to activate its surface for adsorption purposes. Actually, one of the most investigated strategies for the functionalization of cellulose useful for adsorption and/or release of chemicals is based on the grafting of cyclodextrins on the cellulose surface [12]. However the high cost of cyclodextrins and their low grafting yields on cellulose limit the large scale development of this technique. These drawbacks led the research toward the identification of cellulose functionalizing agents different from cyclodextrins.

This work presents glycidyl methacrylate (GMA) as a real alternative to cyclodextrin, as its grafting on cotton fibres allowed us to manufacture adsorbent cellulose materials for the removal of aromatic contaminants from water. GMA has been produced since the early 1990s as a dual functionality monomer for coatings and resins. In the last years cellulose modified materials including GMA have been proposed to remove metals from water [13] and as flame retardant cotton fabric [14]. Withal, plasma graft polymerization of GMA to immobilize cyclodextrins was published by Hirotsu [15] and GMA grafted cellulose films were prepared by operating under ultrasonic irradiation [16].

The GMA grafting on cotton, flax and viscose was previously performed by us following three different cellulose activation strategies, plasma, electron-beam (EB) irradiation and Fenton-type reaction [17]. Afterward, EB activation and the following GMA grafting on cotton, flax, viscose and microcrystalline cellulose have

* Corresponding author.
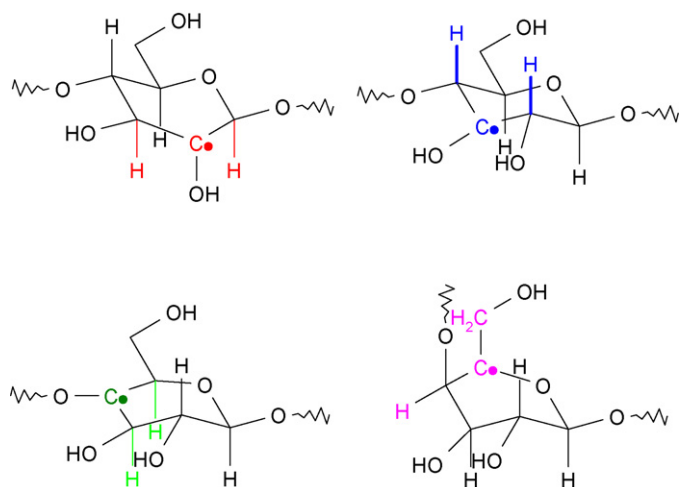 E-mail address: elena.vismara@polimi.it (E. Vismara).

Fig. 1. Typical carbon radicals generated after irradiation of cellulose by high energy e-beams [18].

been extensively investigated [18]. EB irradiation generated different cellulose macroradicals detected by ESR spectroscopy thus supporting a radical GMA grafting mechanism. In Fig. 1 we report some structures of the identified radicals (Fig. 1). From ESR experiments cellulose the macroradicals half life-time was evaluated to be around 24 h.

In the present work the GMA grafting on cotton substrates was performed by the Fenton's reaction [19]. Such approach, more suitable for laboratory scale experiments, allowed preparing two different materials **C1** and **C2**, as summarised in Fig. 2. Both **C1** and **C2** were tested for the removal of phenolic pollutants from aqueous solutions: *phenol* (Ph), *2-naphthol* (BN), *4-nitrophenol* (pNPh), *2,4-dinitrophenol* (dNPh), *2,4,6-trinitrophenol* (tNPh). Many factors, which surely affect the adsorption processes, like the molar substitution ratio (MS) of grafted GMA on the cellulose backbone, the pH and the temperature, were also investigated in detailed kinetic and equilibrium experiments.

2. Experimental

2.1. Materials

Cotton substrates used during this work are common gauzes (10 cm × 10 cm) used for sanitary purposes and purchased in a drug store. All the reagents, H_2O_2, $FeSO_4 \cdot 7H_2O$, glycidyl methacrylate and the aromatic compounds used for the adsorption tests, phenol (Ph), 2-Naphthol (BN), 4-nitrophenol (pNPh), 2,4-dinitrophenol (dNPh) and 2,4,6-trinitrophenol (tNPh) were of reagent grade and used without any other purification. Some physical properties of the selected aromatic compounds are reported in Table 1.

2.2. Adsorbent preparation

In a one-neck round bottom flask (500 mL), cotton gauzes (C0) (6–10 g, 500 mg per gauze), were swelled for half an hour, into 300 mL of H_2O at 80 °C. Then 8 mL of $FeSO_4$ heptahydrate 0.05 M in water were added followed by the addition of 50 mL of H_2O_2 30% (v/v). The mixture was kept for 25 min (*activation time*). After the *activation time*, an amount of GMA (range of 3–6 mL) was added in one portion and accurately stirred to solubilise the monomer, keeping the reaction vessel at the same temperature of the activation process. After 15 min (*quenching time*) the gauzes were removed from the reaction vessel and exhaustively washed five times with 200 mL acetone and finally washed under reflux of acetone for 4 h using an apparatus similar to the Soxhlet extractor. This extensive
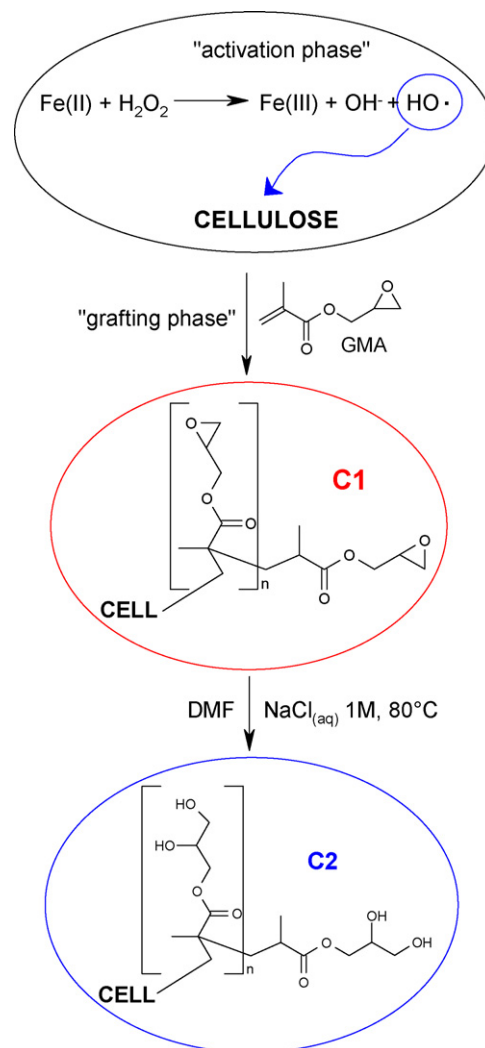

Fig. 2. Simplified representation for the grafting of GMA on cellulose by means of the Fenton's reaction. **C1**: glycidyl form; **C2**: glycerol form.
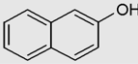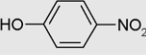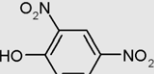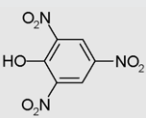
washing procedure has been necessary in order to remove all the GMA homopolymer produced during the reaction and physically covering the surface of the fibres. All the functionalized gauzes (C1) were then squeezed on blotting paper, dried in air and further dried in an oven at 80 °C (ca. 1 h about). Preliminary experiments showed that an activation time longer than 25 min can increase the amount of grafted GMA but a reduction of the mechanical properties of the solid material (brittleness) was observed. Moreover a quenching time of 15 min is sufficient for obtaining the maximum grafting density that is reached just after 10 min.

To obtain the material **C2**, about 3 g of all the samples **C1** were swelled in one-neck round bottom flask (500 mL) with 100 mL of dimethylformamide (DMF) at 80 °C for 2 h. Then, 100 mL of 1 M NaCl aqueous solution were added leaving the reaction mixture under stirring at 80 °C for 24 h. At the end, the samples were removed from the solution and exhaustively washed with water (about 250 mL × 4 times) and finally with acetone (about 100 mL × 2 times). The material was dried before in air and finally in oven at 80 °C (approximately 1 h).

2.3. Adsorption experiments

All the adsorption experiments were performed in batch conditions. Aqueous solutions of the tested aromatic compounds at

Table 1
Pollutants under investigation.

		M_w	Solubility in water at 20 °C (g/100 mL)	pK_a	μ (D)
Ph		94.11	9.48	9.99[a]	1.22[a]
BN		144.17	0.1	9.63[a]	1.0[b]
pNPh		139.11	1.33	7.15[a]	5.27[c]
dNPh		184.11	0.14[*]	4.07[a]	3.02[d] 3.51[e]
tNPh		229.10	1.27	0.42[a]	1.51[d]

[a] Ref. [20].
[b] Calculated. Ref. [21].
[c] Calculated. Ref. [22].
[d] Benzene. Ref. [23].
[e] Dioxane. Ref. [23].
[*] At 54.5 °C.

different concentrations (ranging from 1.0×10^{-4} to 3.0×10^{-3} M for Ph and BN and from 2.0×10^{-5} to 2.4×10^{-3} M for nitrophenols) were prepared diluting a stock solution with deionized water in a 50 mL flask. For nitrophenols the pH was adjusted with 0.5 M HCl or 0.5 M NaOH at values around 2.3 and 11 respectively. 20 mL of the final solution were pipetted in a 25 mL conical flask and then, ca. 50 mg (for nitrophenol batches) or 100 mg (for Ph and BN batches) of functionalized textiles were introduced. All the flasks were shaken at 100 rpm in a thermostatic bath (Julabo SW22) for a time enough to reach the equilibrium.

The concentration of the solutions was determined by UV-spectrophotometer (Jasco V-650) using the data reported in Table 2 for nitrophenols. For BN the molar absorptivity was 1734.3 M^{-1} cm^{-1} at 328 nm. The adsorption capacity was evaluated by the following formula:

$$q = \frac{(C_0 - C) \cdot V}{m} \tag{1}$$

where C_0 and C are, respectively, the initial and the final concentration (M); V is the volume of the solution (L); m is the mass of adsorbent (g).

A further indicator used throughout the work is the removal efficiency, expressed as:

$$\%\text{removal} = \frac{C_0 - C_{eq}}{C_0} \times 100 \tag{2}$$

where C_0 and C_{eq} are, respectively, the initial and equilibrium concentration (M).

Table 2
Wavelengths and UV–vis molar absorptivities.

	pH ∼ 2.3		pH ∼ 11	
	λ (nm)	ε (M^{-1} cm^{-1})	λ (nm)	ε (M^{-1} cm^{-1})
pNPh	317	9717	400	18,376
dNPh	260	12,033	360	14,366
AcPicr	356	14,427	356	14,650

As the samples **C2** are used for the adsorption of nitrophenols at basic pH (∼10–11), and due to the possibility of the hydrolysis of the ester bond in the grafted GMA, a test was performed by soaking about 200 mg of **C2** in 20 mL of NaOH aqueous solution at pH 12 and 25 °C for 48 h. The solid material was washed with water (150 mL × 4 times) and acetone (50 mL × 2 times), and then dried in air before the final characterization.

2.4. Batch desorption

The regeneration of the adsorbents has been fulfilled as follows. With reference to adsorbents previously charged with BN (**C1** and **C2**), samples at different MS were removed from the solutions (C_0 = initial concentration = 5.0×10^{-4} M) and squeezed on blotting paper. Then they were soaked in 30 mL of acetone for 2 h at 30 °C. Acetone was evaporated and the residual solid was dissolved in water. The amount of BN released was determined by UV-spectrometry. With regard to the materials (**C2**) treated with nitrophenols at basic pH (∼11), samples having different MS were removed from the solutions containing the aromatic compounds ($C_0 = 2.0 \times 10^{-4}$ M) and squeezed on blotting paper to remove the excess of liquid. They were introduced in a 25 mL conical flask with 20 mL of water and 500 μL of 0.5 M HCl, and shaken in a thermostatic bath at 30 °C for 24 h. The concentration of the solutions was evaluated by UV-spectrometry. The procedure was repeated different times (up to three times) until a partial or total removal of the adsorbed chemicals.

2.5. Characterization

2.5.1. FT-IR analysis

The solid phase FT-IR spectra of the powdered sample with infrared grade KBr were done by IFS 25 Bruker spectrometer. The ester stretching characteristic signal of the grafted GMA at 1730 cm^{-1} was used to quantify the functionalization. The area of the ester band was normalized with reference to another characteristic cellulose band (780–465 cm^{-1}) as shown by Eq. (3). As reported in previous work [18], the numerical values obtained by Eq. (3) have

a good correlation with the "molar substitution ratio", MS_w, coming out from gravimetric measurements by Eq. (4). MS_w is the average molar ratio between the units of grafted GMA and the units of anhydrous D-glucose:

$$MS_{FT-IR} = area_{N(ester)}$$

$$= \frac{area_{ester}(\text{manual band integration})}{area_{cellulose}(\text{range 780–465 cm}^{-1}\text{ integration})} \quad (3)$$

$$MS_w = \frac{(m - m_0) \cdot 162}{m_0 \cdot 142} \quad (4)$$

In Eq. (4), m and m_0 (g) are, respectively, the final mass and the initial mass of the samples, 162 is the molar mass of D-glucose and 142 is the molar mass of GMA.

2.5.2. CP-MAS ^{13}C solid state NMR

The ^{13}C cross polarization magic angle spinning (CPMAS) spectra were recorded with Bruker ASX 300 spectrometer operating at 75.47 MHz. The following conditions were applied: repetition time 4 s, 1H 90$_-$ pulse length 4.0 µs, contact time 1.2 ms and spin rate 4200 Hz. The compounds were placed in a zirconium rotor, 7 mm in diameter and 21 mm high. The chemical shifts were recorded relative to tetramethylsilane via benzene as a secondary reference.

The crystallinity index (Cr.I.) of **C0** and **C1** has been evaluated by ^{13}C CP MAS spectroscopy as described in [24] throughout the following equation:

$$Cr.I.(\%) = \frac{a}{a+b} \times 100 \quad (5)$$

where a is the C_4 peak area in the range 86–92 ppm and b is the C_4 peak area in the range 80–86 ppm.

2.5.3. Solid state UV-spectrometric analysis

UV–vis spectra of the **C2** solid samples treated with nitrophenols were registered by a Jasco 60 mm integrating sphere working in the range of 200–550 nm (UV/vis band width: 5.0 nm; scan: 400 nm/min; data pitch 0.5 nm). The spectra were analyzed using the instrument software package converting the diffuse reflectance data in absorbance-like data by the Kubelka–Munk equation.

3. Results and discussion

3.1. Functionalization with GMA

The GMA homopolymer produced in the reaction mixture was totally removed from the characterized samples **C1** by extensive washing procedures. The FT-IR spectra of **C0**, **C1** and **C2** are reported in Fig. 3 while the solid state ^{13}C CP MAS spectra of the same samples are showed in Fig. 4. The **C1** spectral characterisations demonstrate the occurrence of the grafting. In the **C1** FT-IR spectra new signals are detectable respect to the regular cellulose skeleton **C0**: 3050–3000 cm^{-1} (weak, C–H epoxide ring stretching), 1730 cm^{-1} (strong, C=O ester stretching), 1270 cm^{-1} and 843 cm^{-1} (C–O–C epoxide ring stretching). These signals identify a glycidyl isobutyrate residue. In the **C1** ^{13}C CP MAS spectrum new signals are detectable respect to the regular cellulose skeleton **C0**. The attributions are shown in Fig. 4. Methyl group, epoxide ring and carbonyl group identify a glycidyl isobutyrate residue. Noteworthy, it is possible to distinguish the CH in the isobutyrate residue directly linked to the cellulose chain from the CH of the epoxy group in the "grafted homopolymer", see Fig. 4. Furthermore, there is no presence of signals related to olefinic carbons which should be located in the range 120–160 ppm between the signal of the carbon C_1 of the cellulose (∼105 ppm) and the signal of the C=O of the ester group (∼178 ppm). This confirms also the absence of unreacted GMA.
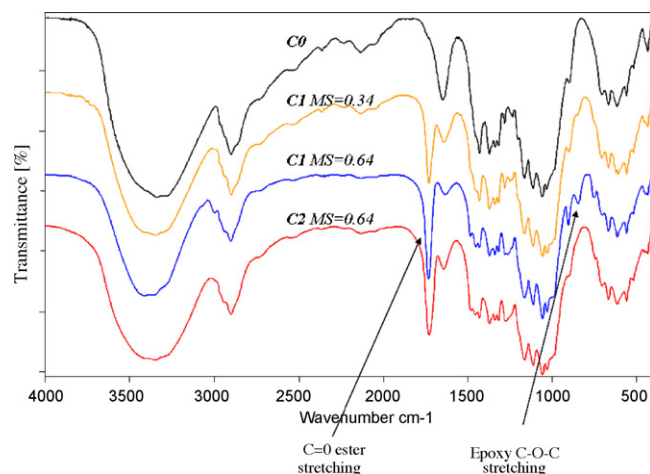

Fig. 3. FT-IR spectra. **C0**: cotton; **C1**: GMA-functionalized cotton (glycidyl form); **C2**: GMA-functionalized cotton (glycerol form).

From the ^{13}C CP MAS spectra it is also possible to see that the grafting procedure does not modify the structure of the cellulose fibres. In particular by ^{13}C CP MAS it was possible to make the calculation of the "crystallinity index" (Cr.I.) related to the percentage of crystalline domains existing in the cellulose fibrils. As reported in the experimental part, Cr.I. was calculated considering the region of the

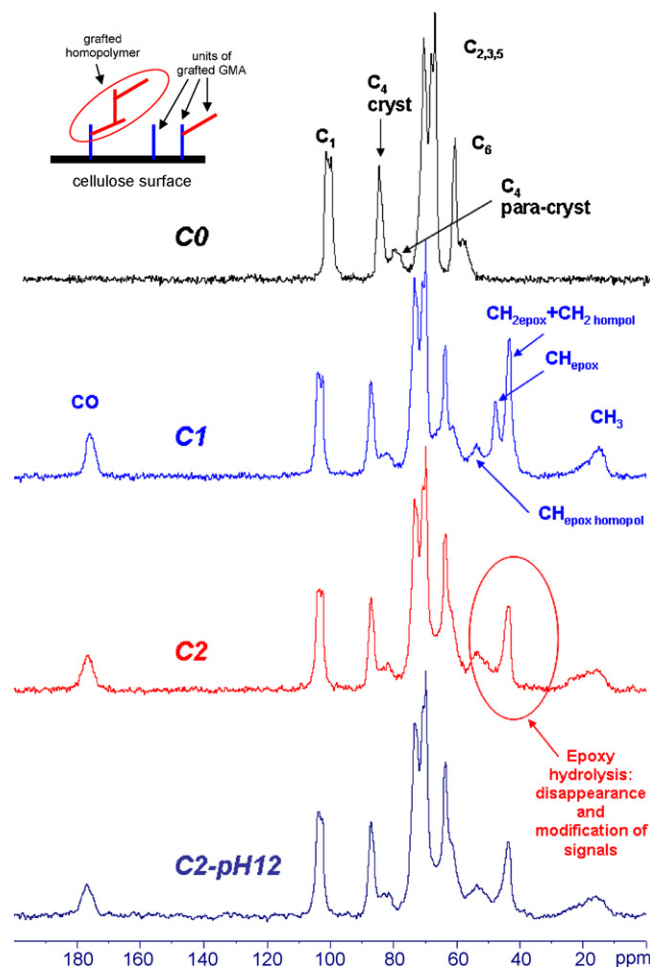

Fig. 4. ^{13}C CP-MAS solid state NMR spectra. **C0**: cotton; **C1**: GMA-functionalized cotton (glycidyl form); **C2**: GMA-functionalized cotton (glycidyl form); **C2-pH 12**: **C2** sample treated with NaOH$_{(aq)}$ pH 12, 25 °C, 48 h.
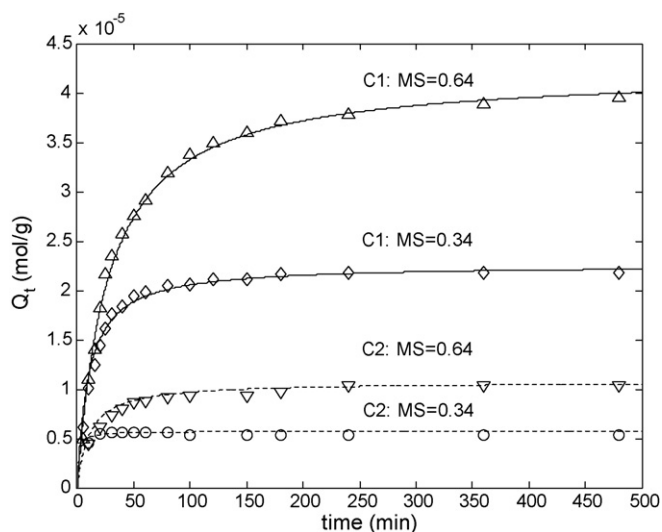
Fig. 5. Plot of Q_t vs. time for the adsorption of BN on **C1** and **C2** samples at different MS, $C_0 = 5E-4M$; $T = 25\,°C$; ($\diamond$) **C1**: MS = 0.34; ($\triangle$) **C1**: MS = 0.64; ($\bigcirc$) **C2**: MS = 0.34; ($\triangledown$) **C2**: MS = 0.64.

^{13}C CP MAS associated to the carbon C$_4$ of the glucose units of the cellulose polymer chain. Such region is characterized by the presence of an up-field wing which is given due the presence of less ordered domains in the cellulose fibrils. For the non-derivatized cotton **C0** a Cr.I. around 63% was found and this value is not substantially modified after the GMA grafting.

The transformation from **C1** to **C2** by hydrolysis of the epoxide ring causes a modification of both the FT-IR and ^{13}C CP MAS spectra by the disappearance of the epoxy group signals. The signals of the ester carbonyl group were unchanged.

The **C2** sample treated with the NaOH solution for testing the maintenance of the ester bond was also analyzed by FT-IR (not reported) and ^{13}C CP MAS (Fig. 4). No degradation of the grafted GMA and of the cellulose structure was observed.

3.2. Adsorption of phenol and 2-naphthol

3.2.1. Kinetic data

For Ph no adsorption data are available because this molecule is not adsorbed both by **C1** and by **C2** at any pH. Experiments performed using **C1** and **C2** substrates at different MS, soaked in solutions of Ph at different concentrations and at different pH conditions (from 2 up to 11) did not show any adsorbent property related to the two functionalized materials. Instead, the kinetic data of BN adsorption on **C1** and **C2** and the effect of the MS are depicted in Fig. 5. The amount (moles) of BN adsorbed per gram of adsorbent, Q_t (mol/g), is reported versus the time (min) at $T = 25\,°C$ and for an initial concentration of 5.0×10^{-4} M.

The graph shows that BN is adsorbed better on **C1** than on **C2**: **C1** adsorbs BN almost four times more than **C2**. This happens because, being BN a hydrophobic molecule with a weak dipole moment and a low water solubility, it is more efficiently adsorbed on substrates like **C1** less hydrophilic than **C2**. Moreover a proportionality

between the MS and the amount of adsorbed BN is evidenced: for example, passing from MS = 0.33 to MS = 0.6, Q_e (moles of BN adsorbed at equilibrium, mol/g) moves from ca. 2.0×10^{-5} mol/g to ca. 4.0×10^{-5} mol/g for **C1**. In order to find the kinetic model for the adsorption process, the experimental data were correlated with the pseudo-first-order and pseudo-second-order models [25]. The pseudo-first-order expression, in the integral form, is:

$$\ln(Q_{e1} - Q_t) = \ln Q_{e1} - k_1 t \tag{6}$$

The pseudo-second-order kinetic model could be expressed (always in the integral form) as:

$$\frac{t}{Q_t} = \frac{1}{k_2 Q_{e2}^2} + \frac{t}{Q_{e2}} \tag{7}$$

In such equations, k_1 is the pseudo-first-order rate constant (min^{-1}) and k_2 is the pseudo-second-order rate constant (g/(mol min)). By using Eq. (6) and Eq. (7) we obtained the data reported in Table 3. The second-order model fits the data very well while the first-order model is quite inappropriate for the analysis of the process. In particular the second-order model can be applied to both **C1** and **C2** at different MS. In any case, the equilibrium amounts of adsorbed BN calculated by the second-order equation are consistent with experimental data and the correlation coefficients are near the unity. The second-order rate constant decreases when the MS increases. This could be explained with the dependence of k_2 by a diffusive transport resistance into the functional layer of grafted-GMA created on the cellulose surface and by the fact that the higher is the value of the MS the wider is the thickness of the layer.

3.3. Adsorption of 2-naphthol

3.3.1. Equilibrium data

The equilibrium isotherms for the BN adsorption on **C1** at different temperatures (25, 35 and 45 °C) and MS have been determined and reported in Fig. 6. Two of the most used models in literature for the analysis of the equilibrium isotherms are the Langmuir and the Freundlich models. They can be described by Eq. (8) and Eq. (9) respectively, where Q_e (mol/g) is the amount of substance adsorbed at equilibrium on the solid phase and C_{eq}(M) is the concentration of the solution at equilibrium. In the Langmuir model, Q_m (mol/g) is the maximum adsorption capacity while b is a constant related to the energy of adsorption. It is valid in the ideal conditions of a fully uniform adsorption surface, absence of interactions between adsorbed molecules and formation of a monolayer at the maximum adsorption capacity [26]. In the Freundlich equation, K_F is the Freundlich constant and n is a constant related to the intensity of adsorption (heterogeneity factor): values of $n > 1$ are related to a favourable physical adsorption while for values of $n < 1$ the adsorption process is chemical. The Freundlich model is valid in the case of multilayer adsorption with interactions between adsorbed molecules and heterogeneous adsorption surfaces with a non-uniform distribution of the heat of adsorption [26].

$$Q_e = \frac{Q_m b C_{eq}}{1 + b C_{eq}} \tag{8}$$

$$Q_e = K_F C_{eq}^{1/n} \tag{9}$$

Table 3
Kinetic parameters for the adsorption of BN on **C1** at different MS. $C_0 = 5E-4M$; $T = 25\,°C$.

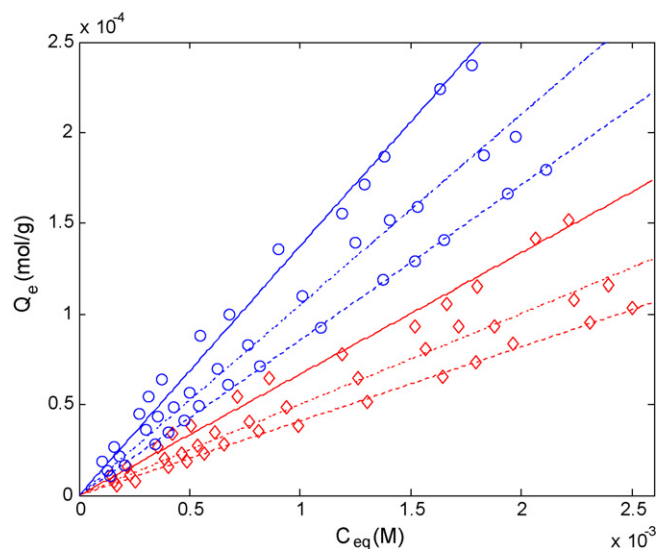|	MS	$Q_{e,exp}$ (mol/g)	Pseudo-first-order			Pseudo-second-order		
			k_1 (min^{-1})	$Q_{e,cal}$ (mol/g)	R^2	k_2 (g/(mol min))	$Q_{e,cal}$ (mol/g)	R^2
C1	0.34	2.70E−5	2.52E−2	1.16E−5	0.9464	4404	2.26E−5	0.9996
C1	0.64	4.50E−5	1.12E−2	2.34E−5	0.9523	876	4.22E−5	0.9988
C2	0.34	5.40E−6	2.0E−6	1.63E−5	0.0002	131,890	5.73E−6	0.9992
C2	0.64	1.03E−5	4.0E−4	3.24E−5	0.5738	8785	1.07E−5	0.9988

Fig. 6. Adsorption isotherms for BN on **C1** at different MS, Contact time, 24 h; (◇) MS = 0.34, (○) MS = 0.64; continuous line, 25 °C; dash-dot line 35 °C; dashed line, 45 °C.

From Eq. (8), if $bC_{eq} \ll 1$ then $Q_e = Q_m bC_{eq} = K'C_{eq}$, that is the nonlinear Langmuir model become a linear model for values of concentration $C_{eq} \ll 1/b$. On the other hand Freundlich model can also become linear when $n = 1$.

By visual inspection of the experimental data, the relation Q_e vs. C_{eq}, seems to be linear in the range of concentrations investigated. This suggests that if Langmuir model were valid our data can be analyzed only by the linear part of the Langmuir relation and if Freundlich model were valid the parameter n should be equal to or near to the unity. For this reason it is not convenient to make predictions on the parameters of both models because the scarce nonlinearity of the data can lead toward misleading conclusions when regression models are used. The best we can do is to use the simple linear equation $Q_e = K'C_{eq}$ and evaluating the parameter K'. It is noteworthy that there is an upper bound for the max concentration of BN in water linked to its low solubility in this solvent (0.074 g in 100 mL (5.132×10^{-3} M) at 25 °C). In our case, the maximum equilibrium concentrations C_{eq} are around 2.0 to 2.5×10^{-3} M (the highest initial concentration of BN considered in this work is 3.0×10^{-3} M).

In Table 4, the equilibrium constants $K' = Q_e/C_{eq}$ are reported for different temperatures (25, 35 and 45 °C) and MS. The reduction of the adsorption capacity and, therefore, of the equilibrium constant with the increasing of the temperature is indicative of the exothermicity of the process. However quantitative information on the thermodynamic of the process can be obtained from the well-known relation:

$$\ln K = \frac{\Delta S^\circ}{R} - \frac{\Delta H^\circ}{RT} \tag{10}$$

Table 4
Values of the equilibrium constant $K' = q_e/C_{eq}$ for BN adsorption on **C1** at different MS and temperature. Contact time: 24 h.

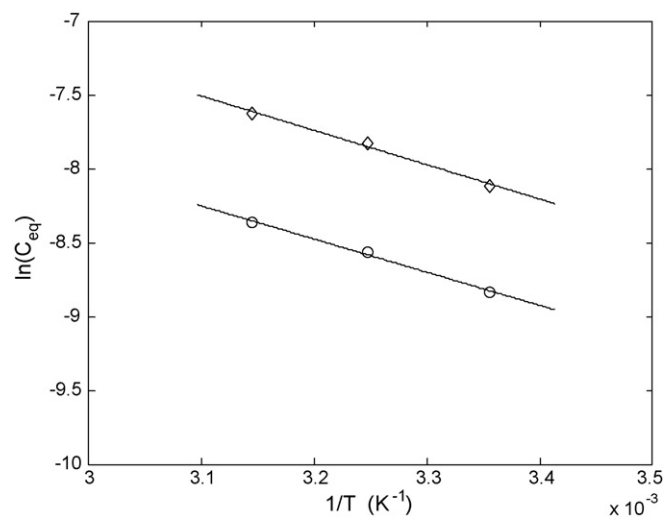| MS	T (°C)	K' (L/g)	R^2
	25	0.0669	0.9884
0.34	35	0.0502	0.9933
	45	0.0410	0.9969
	25	0.1374	0.9869
0.64	35	0.1051	0.9937
	45	0.0856	0.9991

Fig. 7. Adsorption of BN on **C1**. Plot of $\ln C_{eq}$ vs. $1/T$ for the evaluation of the thermodynamics data. (◇) MS = 0.34; (○) MS = 0.64.

where K is the equilibrium constant, ΔH° and ΔS° are the enthalpy (in $J\,mol^{-1}$) and entropy change (in $J\,K^{-1}\,mol^{-1}$) respectively, R is the universal gas constant ($8.314\,J\,K^{-1}\,mol^{-1}$) and T is the absolute temperature (in K). The equilibrium constant K is only function of the temperature and is related to the composition of the system by the relation [27]:

$$K = \frac{a_{ads}}{a_{sol}} = \frac{\chi_{ads} Q_e}{\chi_{sol} C_{eq}} \tag{11}$$

where a_{sol} and a_{ads} are the equilibrium activities of the compound in solution and on the solid phase respectively, χ_{sol} and χ_{ads} their activity coefficients, C_{eq} is the equilibrium concentration in solution (M) and Q_e is the equilibrium adsorbate concentration on the sorbent (mmol/g). In the case of dilute system (i.e. $C_{eq} \to 0$) the activity coefficients move toward the unity so the Eq. (11) can be approximate by the following:

$$K \cong K' = \frac{Q_e}{C_{eq}} \tag{12}$$

By Eqs. (10) and (11) it is possible relate ΔH° and ΔS° to C_{eq} and Q_e [28]:

$$\ln C_{eq} = \left(\ln Q_e - \frac{\Delta S^\circ}{R} \right) + \frac{\Delta H^\circ}{R} \frac{1}{T} \tag{13}$$

Thus, $\ln C_{eq}$ values for a fixed Q_e are plotted against $1/T$ (in the Eq. (13), the units of Q_e are mmol/g if C_{eq} is expressed in mol/L). The slope and intercept of a regression line fitting the data can be used for the evaluation of the thermodynamic parameters. Due to the linear relationship between C_{eq} and Q_e for the BN adsorption on **C1** in the range of C_{eq}, 0 to 2.5×10^{-3} M, an arbitrarily value of Q_e can be chosen. Calculating by Eq. (13) the corresponding values of C_{eq} for three different temperatures (25, 35 and 45 °C) it is possible obtain the data reported in Fig. 7. A linear regression gives three values of ΔH° and ΔS°. In particular it is possible to find $\Delta H^\circ \cong -20$ kJ/mol. Such low value is indicative of a reversible physical adsorption process. Moreover $\Delta S^\circ \cong -30$ J/mol K and the negative sign is in agreement with the physical nature of the process: BN molecules adsorbed on the solid phase are in a more ordered state than in solution phase. Finally $\Delta G^\circ = \Delta H^\circ - T\Delta S^\circ \cong -12$ kJ/mol. The negative sign is indicative of the spontaneity of the process. All the thermodynamic data are reported in Table 5. The reversibility of the process has been evidenced during BN desorption experiments: using acetone as solvent it is possible remove around 90–95% of the uploaded BN. It is worthwhile to remember at this point that

Table 5
Adsorption of BN on **C1**. Thermodynamic data.

MS	Q_e (mmol/g)	$\Delta H°$ (kJ/mol)	$\Delta S°$ (J/(mol K))	$\Delta G°$ (kJ/mol)		
				298 K	308 K	318 K
0.34	2.0E−2	−19.31	−29.96	−10.37	−10.08	−9.78
0.64	2.0E−2	−18.65	−21.75	−12.17	−11.95	−11.74

the desorption of BN using acetone has been pursued only in order to have the experimental confirmation of the reversibility of the adsorption process. Obviously the use of acetone, as well as any other organic, solvents does not seem to be suitable for the regeneration of such filters in the industrial contest. Pure water could also be used due to the reversibility of the process but the release time is to much long for practical measurements.

3.4. Adsorption of nitrophenols

3.4.1. Kinetic data

Fig. 8 shows the influence of the pH on the kinetic of adsorption of the three nitrophenols on **C2** at MS = 0.64 and at the temperature of 25 °C. It is evident that the pH has a strong influence on the adsorption capacity of the materials: basic pH (~11) is suitable for the removal of all three species while acidic pH (~2.3) reduces considerably the amount of pNPh and dNPh uploaded on the adsorbent. The removal efficiency, as described by Eq. (2), reaches ca. 70% for pNPh, ca. 84% for dNPh and ca. 95% for tNPh at pH 11 when $C_0 = 2.0 \times 10^{-4}$ M and $T = 25$ °C. Instead when the pH is reduced around 2.3 only tNPh is efficiently removed (ca. 93%) while for pNPh and dNPh the removal percentage falls to about 3% and 17% respectively. Using Eqs. (6) and (7) it is possible to find the kinetic model of the process. As it can be seen from Table 6 the experimental data fit very well with the pseudo-second-order model in both pH conditions (R^2 is always near the unity and the calculated adsorption capacity $Q_{e,cal}$ is consistent with the experimental data) while the first-order model seems not be very reliable. The differences between the values of the second-order adsorption rate constant k_2 at pH 2.3 and pH 11 for pNPh and dNPh is, in part, due to the reduced amount of adsorbed compound in acidic conditions (a shorter time is necessary for reaching the equilibrium). Instead for tNPh, both k_2 values have the same order of magnitude (195.63 g/mol min at pH 11 and 205.9 g/mol min at pH 2.3). Moreover, the calculated adsorption capacity $Q_{e,cal}$ for tNPh has similar values in both pH conditions (7.143×10^{-5} mol/g at pH 11 and 6.944×10^{-5} mol/g at pH 2.3). A possible explanation of this result is that the three nitroaromatic compounds are removed from the solution when they are in the saline form. In fact, at low pH, pNPh and dNPh are practically in the undissociated form. The ratio [A−]/[HA] between the concentrations of the anionic and molecular forms is reported in Table 7: it is around 10^{-5} for pNPh and 10^{-2} for dNPh. Instead, the same ratio is around 50 for tNPh. This means that, at pH 2.3, tNPh is already enough dissociated due to its low pK_a.

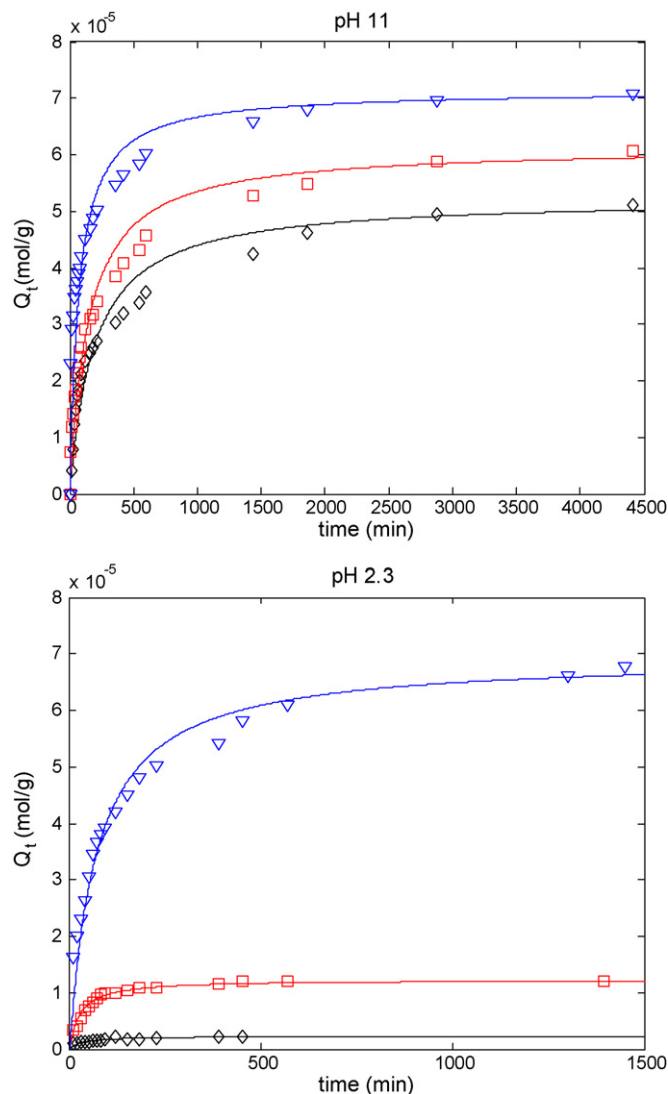**Fig. 8.** Adsorption kinetics of nitrophenols on **C2**. Influence of pH. $C_0 = 2.0E-4M$; $T = 25$ °C; MS = 0.64; (◇) pNPh; (□) dNPh; (▽) tNPh.

Table 6
Kinetic parameters for the adsorption of nitrophenols on **C2** at different pH. $C_0 = 2.0-4M$; $T = 25$ °C; MS = 0.64.

	pH	$Q_{e,exp}$ (mol/g)	Pseudo-first-order			Pseudo-second-order		
			k_1 (min^{-1})	$Q_{e,cal}$ (mol/g)	R^2	k_2 (g/(mol min))	$Q_{e,cal}$ (mol/g)	R^2
pNPh	11	5.11E−5	0.0011	3.47E−5	0.9706	99.08	5.24E−5	0.9964
	2.3	2.18E−5	7.0E−5	6.47E−5	0.3504	13735	2.31E−6	0.9915
dNPh	11	6.06E−5	0.0011	3.91E−5	0.9591	110.11	6.14E−5	0.9977
	2.3	1.20E−5	3.0E−5	7.39E−5	0.6851	3029.5	1.23E−5	0.9995
AcPicr	11	7.08E−5	0.0013	3.22E−5	0.9523	195.63	7.14E−5	0.9993
	2.3	7.42E−5	0.0012	4.00E−5	0.8479	205.9	6.94E−5	0.9988

Table 7
Ratios [A$^-$]/[HA] between the anionic form and the molecular form of nitrophenols at different pH and initial concentration [HA]$_0$.

	pK_a	pH 2.3		pH 11	
		[HA]$_0$ = 2E−4M	[HA]$_0$ = 2E−3M	[HA]$_0$ = 2E−4M	[HA]$_0$ = 2E−3M
pNPh	7.15	~1.5E−5	~1.5E−5	∞	∞
dNPh	4.07	~2.0E−2	~1.5E−5	∞	∞
tNPh	0.42	~75	~55	∞	∞
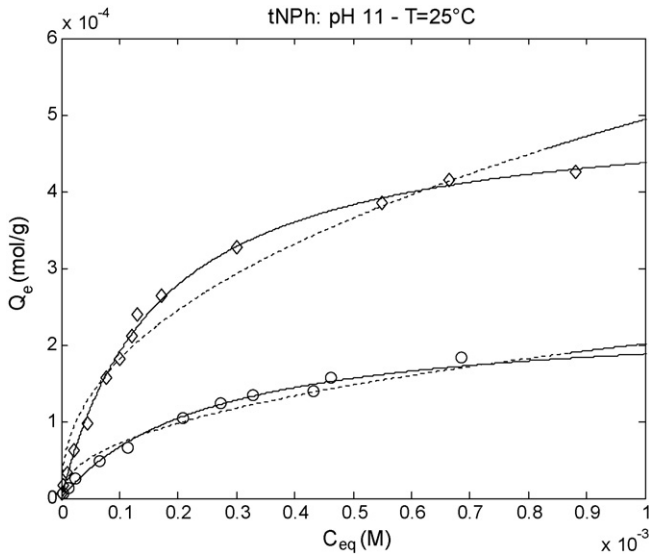
Fig. 9. Adsorption isotherms of tNPh on **C2** (pH 11). Influence of MS. (○) MS = 0.34; (◊) MS = 0.64; continuous line: Langmuir; dashed line: Freundlich; contact time 60 h; T = 25 °C.
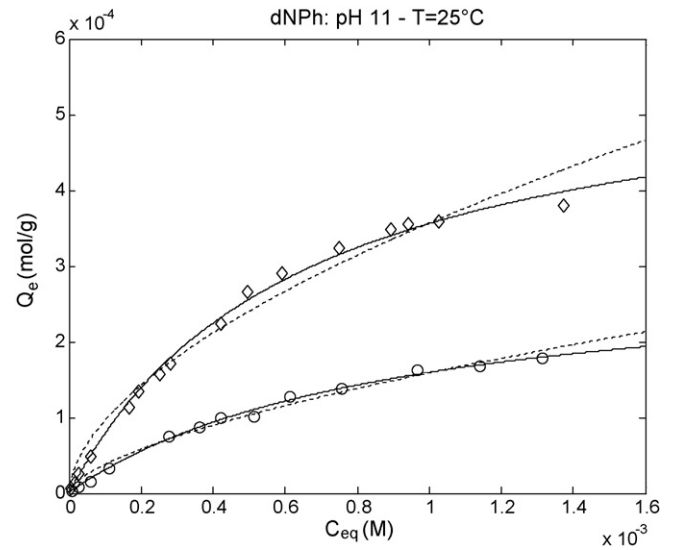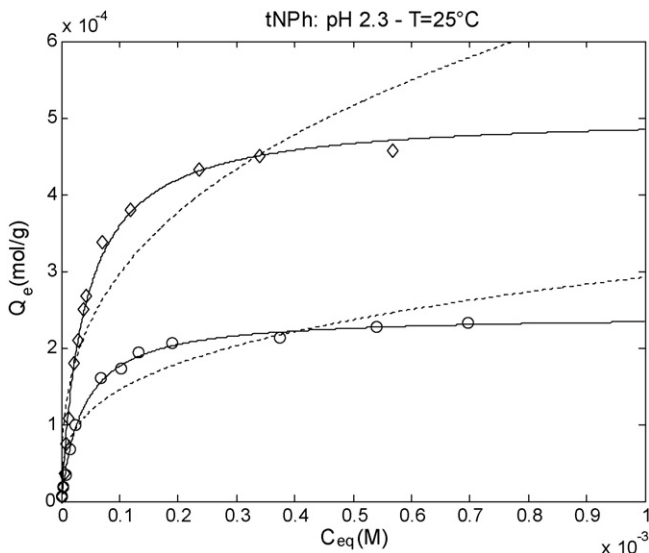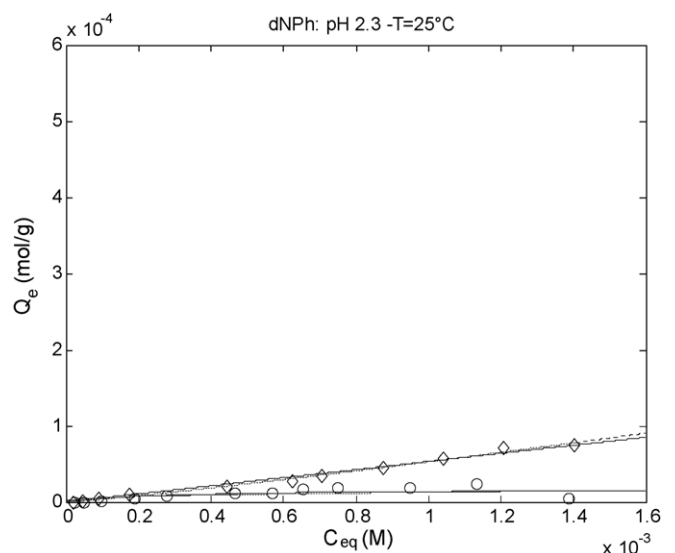

Fig. 11. Adsorption isotherms of dNPh on **C2** (pH 11). Influence of MS. (○) MS = 0.34; (◊) MS = 0.64; continuous line: Langmuir; dashed line: Freundlich; contact time 60 h; T = 25 °C.

3.5. Adsorption of nitrophenols

3.5.1. Equilibrium data

The adsorption isotherms at 25 °C for the three nitrophenols pNPh, dNPh and tNPh on **C2** at two different grafting levels (MS) and pH conditions are reported in Figs. 9–13. The Langmuir and Freundlich models have been used for fitting the experimental data by least squares nonlinear regression using the software Mat-

lab. Even if linear regression applied to the linearly transformed isotherm equations is the most used technique for the evaluation of the model parameters, the transformation of Eq. (8) and Eq. (9) from nonlinear to linear [29] can modify the distribution of the errors and in some cases can lead toward wrong predictions [30–33]. The effect of the MS on the adsorption capacity is quite evident for all three aromatic compounds: higher MS are associated with a higher amount of uploaded compound. On the other

Fig. 10. Adsorption isotherms of tNPh on **C2** (pH 2.3). Influence of MS. (○) MS = 0.34; (◊) MS = 0.64; continuous line: Langmuir; dashed line: Freundlich; contact time 60 h; T = 25 °C.

Fig. 12. Adsorption isotherms of dNPh on **C2** (pH 2.3). Influence of MS. (○) MS = 0.34; (◊) MS = 0.64; continuous line: Langmuir; dashed line: Freundlich; contact time 60 h; T = 25 °C.
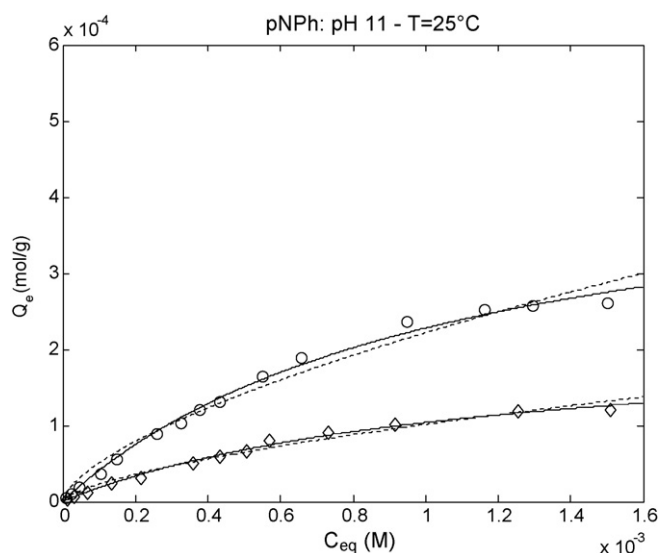
Fig. 13. Adsorption isotherms of pNPh on **C2** (pH 11). Influence of MS. (○) MS = 0.34; (◇) MS = 0.64; continuous line: Langmuir; dashed line: Freundlich; contact time 60 h; $T = 25\,^\circ$C.
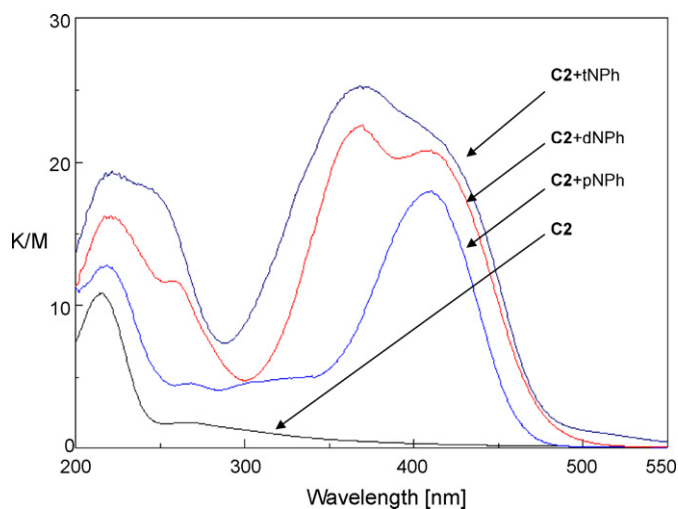

Fig. 14. Solid state UV–vis spectra by 60 mm integrating sphere of **C2** samples treated with nitrophenols (pH 11).
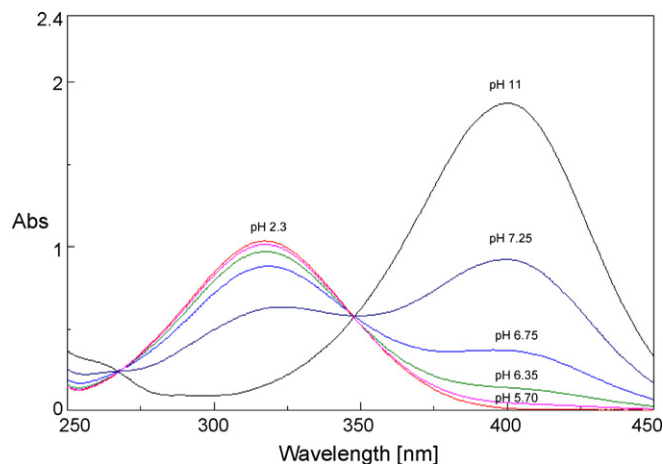

Fig. 15. UV–vis spectra of pNPh aqueous solutions at different pH. $C_0 = 1 \times 10^{-4}$ M.

hand, a very strong dependence from the pH has been recognized: all three nitrophenols are efficiently removed from solutions at basic pH (Figs. 9, 11 and 13) while only tNPh can be removed from acidic solutions (Fig. 10). In both pH conditions, the data can be well fitted by Langmuir equation. All the calculated parameters are reported in Table 8. The maximum upload Q_m depends by MS and has the same order of magnitude ($\sim 2.5 \times 10^{-4}$ mol/g for MS = 0.35 and $\sim 5.0 \times 10^{-4}$ mol/g for MS = 0.64) for all three nitro-aromatic compounds in both pH conditions. Instead, the parameter b, linked to the adsorption energy and, therefore, to the equilibrium constant, strongly depends from the number of nitro groups on the aromatic molecule and from the MS. With reference to tNPh, an increase of the b values (around ten times more) occurs also passing from pH 11 to pH 2.3. As pointed out also by kinetic data, pNPh can be adsorbed on **C2** only when the pH is basic (Fig. 13), that is when pNPh is in its saline form, but not at low pH where pNPh can be considered totally undissociated. For this reason, adsorption data for pNPh on **C2** at pH 2.3 are not reported. With reference to dNPh, **C2** shows a very weak capacity of removal at pH 2.3 (Fig. 12) and only materials having high MS are able to remove a significant amount of dNPh in acidic conditions. For this reason, working at pH 2.3 a great care should be taken in making measurements mainly at low MS: large errors can come out due to the reduced amount of dNPh adsorbed on the solid phase. For this reason, the lines used for fitting the dNPh data at pH 2.3 (Fig. 12) with reference to both models, Langmuir and Freundlich are just reported for completeness, and should be used only for a better visualization of the data on the graph and not for making predictions.

Table 8
Langmuir and Freundlich constants for pNPh, dNPh and tNPh adsorption on **C2** at different MS and pH. $T = 25\,^\circ$C; contact time 60 h.

			Langmuir model			Freundlich model		
			Q_m (mol/g)	b	R^2	K_F	n	R^2
MS = 0.34	pH 2.3	pNPh	a	a	a	a	a	a
		dNPh	b	b	b	b	b	b
		tNPh	2.43E−4	2.62E+4	0.9992	2.39E−3	3.29	0.9708
	pH 11	pNPh	2.21E−4	0.89E+3	0.9979	8.92E−3	1.54	0.9928
		dNPh	3.02E−4	1.13E+3	0.9989	1.19E−2	1.60	0.9955
		tNPh	2.36E−4	3.95E+3	0.9977	4.52E−3	2.22	0.9870
MS = 0.64	pH 2.3	pNPh	a	a	a	a	a	a
		dNPh	b	b	b	b	b	b
		tNPh	5.08E−4	2.48E+4	0.9984	7.03E−2	2.91	0.9637
	pH 11	pNPh	4.71E−4	0.94E+3	0.9980	1.89E−2	1.55	0.9595
		dNPh	5.86E−4	1.55E+3	0.9989	1.85E−2	1.75	0.9932
		tNPh	5.11E−4	5.99E+3	0.9993	1.00E−2	2.30	0.9881

a No adsorption.
b Very weak adsorption.

Table 9

Release of nitrophenols from **C2** at different MS; for every batch, 20 mL H_2O + 500 µL HCl 0.5 M; T = 30 °C. All sample were previously charged in basic conditions (pH 11; C_0 = 2E−4M; T = 25 °C).

	Adsorbed amount (mol/g)	1st Release	2nd Release	3rd Release	Cumulative release (%$_{mol/mol}$)		
		%$_{mol/mol}$	%$_{mol/mol}$	%$_{mol/mol}$	20 mL water	40 mL water	60 mL water
tNPh							
MS = 0.34	4.75E−5	11.07	8.87	6.94	11.07	19.94	26.88
MS = 0.64	6.05E−5	4.72	4.36	3.70	4.72	9.08	12.78
dNPh							
MS = 0.34	3.03E−5	80.81	4.66	∼0	80.81	85.47	85.47
MS = 0.64	4.82E−5	67.23	6.53	0.71	67.23	73.76	74.47
pNPh							
MS = 0.34	1.46E−5	70.94	2.9	∼0	70.94	73.84	73.84
MS = 0.64	4.33E−5	82.43	2.45	∼0	82.43	84.88	84.88

The adsorption of the nitrophenols in their saline forms has found an experimental confirmation by the solid state UV–vis spectra of the charged **C2** samples, obtained using a 60 mm integrating sphere. In Fig. 14 the spectra of **C2** with and without adsorbed nitrophenols are reported. The vertical axis is reported in absorbance-like units (K/M) after the conversion of the diffuse reflectance data using the Kubelka–Munk equation. While the spectrum of pure **C2** has no relevant peaks in the range of wavelengths investigated, the spectrum of **C2** charged with pNPh has a relevant peak around 400 nm (∼408 nm) that is typical of the p-nitrophenate ion in agreement with the yellow colour of the textile sample charged with pNPh. The same peak (∼400 nm) is present in the UV–vis spectrum of the aqueous solution of pNPh at basic pH, while at acid pH a different spectral profile with a peak at 317 nm is observed (Fig. 15). In the same figure it is evidenced also the great sensibility of the UV–vis spectrum of pNPh to the pH modification in the range 5.5–7.5. Such sensibility can affect the reliability of the measurements made in that range and justify the need of working at low (∼2) and high pH (∼11). Obviously, as the maximum adsorption capacity is reached at high pH while there is no removal (or very low) at low pH, the adsorption capacity of **C2** toward pNPh at intermediate pH (5.5–7.5) lies in between the two extremes. The same experimental evidences have been found for dNPh: the solid state UV–vis spectrum of **C2** charged with dNPh has a relevant peak around 365 nm and the spectrum of the aqueous solution of dNPh at basic pH show the same profile with a peak around 360 nm, while the spectrum of the aqueous solution of dNPh at acid pH is quite different and has a peak at 261 nm. Finally the spectrum of **C2** charged with tNPh shows a peak around 368 nm. The corresponding spectrum of the tNPh aqueous solution at basic pH has a similar profile with a major peak at 356 nm. For tNPh there are few variations between the aqueous solution spectra at different pH, basic (∼11) and acid (∼2), because, due to the low value of picric acid pK_a (see Table 1), in both conditions tNPh is largely dissociated. UV–vis spectra of dNPh and tNPh in aqueous solution have not been reported in this work.

3.6. Desorption of nitrophenols

Table 9 shows the data of desorption of nitrophenols from **C2** at different MS (0.34 and 0.64) in acidic conditions and at T = 30 °C. All sample (ca. 50 mg) have been previously charged with nitrophenols in basic conditions (pH 11) at the initial concentrations C_0 = 2.0 × 10^{-4} M and at T = 25 °C. The amount of nitrophenols adsorbed on **C2** is also reported in Table 9. After a 24 h desorption time the concentration of the solution is measured by UV-spectrophotometer. If the adsorbent has not released all the adsorbed compound, the desorption procedure is repeated again, as described in the experimental part, until the instrument is able to detect a valuable signal. From the data it is possible to see

that pNPh is easily desorbed from the solid substrate using a low-pH solution. Only 20 mL of acid aqueous solution are enough to remove around 85–90% of the adsorbed compound from 50 mg of adsorbent. This observation is in agreement with the adsorption data from which it is evident that pNPh can be adsorbed on **C2** mostly when the pH is basic, that is when pNPh is in its anionic form and very less when the pH is acid, which is when pNPh is in the molecular form. Passing from pNPh to dNPh the effect of pH changing on the desorption is still evident. Nevertheless it is necessary to repeat the desorption procedure two or three times needing so a higher volume of acid solution. Moreover the cumulative removal percentage decreases with the increase of the MS. This is also consistent with the adsorption data because materials with higher MS have a higher capacity of holding adsorbed molecules on their surface. Finally, the data for tNPh show that the desorption in acidic conditions is very weak. After three washing steps (60 mL of total volume required) only 25–26% is removed from a material with MS = 0.34 while the percentage reduces at 12–13% for a MS = 0.64.

4. Conclusion

The synthesis and the characterization of new functional cellulosic textiles, **C1**, have been worked up by grafting glycidyl methacrylate on the cellulose fibres by the Fenton's reaction. **C1** can be further modified by the opening of the epoxy ring in the glycidyl group through a solvolysis reaction (**C2**). Both materials **C1** and **C2** have been tested for the removal of aromatic pollutants from water. The influence of the "molar substitution ratio", related to the amount of the grafted GMA on the cellulose fibres, on the adsorption properties has been found as relevant. Functionalized textiles **C1** supporting glycidyl groups are able to adsorb hydrophobic molecules like BN while derivatized cellulose substrates **C2** having glycerol groups show higher affinity toward hydrophilic molecules like nitrophenols. In this case, the presence and the number of the nitro groups is essential for the adsorption of such molecules. In fact phenol is not adsorbed at all, either by **C1** or by **C2** at any pH condition. The acidity of the OH group, which depends on the number of nitro groups, seems to play a fundamental role on the adsorption mechanisms. In fact, the adsorption capacity of nitrophenols depends strongly upon the pH of the solution: pNPh, dNPh are better adsorbed in basic solutions (pH ∼ 10–11), while only tNPh can efficiently be removed both in acid (pH ∼ 2) and in basic environments. No degradation of **C2** has been observed after **C2** treatment with NaOH aqueous solutions. With regard to the dependence of the nitrophenol adsorption efficiency to the pH of the aqueous solutions, it is possible to consider the regeneration of **C2** filters using aqueous HCl solutions for the nitrophenols desorption. In this case, as their negative environmental impact is well-known, industrial applications of **C2** is very promising due to

the possibility of maximizing the removal efficiency, working at high pH and regenerating the adsorbent simply by only reducing the pH. For this reason, the application of **C2** as adsorbent filter could be pursued through an integrated strategy of wastewater treatment: **C2** filters can be used in order to remove nitrophenols at low concentration from high volumes of water. The regeneration of the adsorbents by using acidulated water allows the release of the adsorbed molecules generating a more concentrated aqueous solution. This reduces drastically the volumes of water to be treated using other treatment technologies.

References

[1] R. Andreozzi, A. D'Apuzzo, R. Marotta, A kinetic model for the degradation of benzothiazole by Fe^{3+} photo-assisted Fenton process in a completely mixed batch reactor, J. Hazard. Mater. B80 (2000) 241–257.

[2] M.A. Oturan, J. Peiroten, P. Chartrin, A.J. Acher, Complete destruction of p-nitrophenol in aqueous medium by electro-Fenton method, Environ. Sci. Technol. 34 (2000) 3474–3479.

[3] P. Canizares, C. Saez, J. Lobato, M.A. Rodrigo, Electrochemical treatment of 2,4-dinitrophenol aqueous wastes using boron-doped diamond anodes, Electrochim. Acta 49 (2004) 4641–4650.

[4] S. Yi, W. Zhuang, B. Wu, S.T. Tay, J. Tay, Biodegradation of p-nitrophenol by aerobic granules in a sequencing batch reactor, Environ. Sci. Technol. 40 (2006) 2396–2401.

[5] C. Yang, Y. Qian, L. Zhang, J. Feng, Solvent extraction process development and on-site trial-plant for phenol removal from industrial coal-gasification wastewater, Chem. Eng. J. 117 (2006) 179–185.

[6] U.K. Ghosh, N.C. Pradhan, B. Adhikari, Synthesis and characterization of porous polyurethaneurea membranes for pervaporative separation of 4-nitrophenol from aqueous solution, Bull. Mater. Sci. 29 (2006) 225–231.

[7] A.T. El-Gendi, S.A. Ahmed, H.A. Talaat, Preparation and evaluation of flat membranes for phenols separation, Desalination 206 (2007) 226–237.

[8] T. Dengyong, Z. Zheng, L. Kui, L. Jingfei, Z. Jibiao, Adsorption of p-nitrophenol from aqueous solutions onto activated carbon fiber, J. Hazard. Mater. 143 (2007) 49–56.

[9] C. Moreno-Castilla, J. Rivera-Utrilla, M.V. López-Ramón, F. Carrasco-Marín, Adsorption of some substituted phenols on activated carbons from a bituminous coal, Carbon 33 (6) (1995) 845–851.

[10] B. Pan, W. Du, W. Zhang, X. Zhang, Q. Zhang, B. Pan, L. Lv, Q. Zhang, J. Chen, Improved adsorption of 4-nitrophenol onto a novel hyper-cross-linked polymer, Environ. Sci. Technol. 41 (2007) 5057–5062.

[11] G. Crini, Non-conventional low-cost adsorbents for dye removal: a review, Bioresour. Technol. 97 (2006) 1061–1085.

[12] J. Szejtli, Cyclodextrins in the textile industry, Starch 55 (2003) 191–196 (and references therein).

[13] T.S. Anirudhan, S. Jalajamony, L. Divya, Efficiency of amine-modified poly(glycidyl methacrylate)-grafted cellulose in the removal and recovery of vanadium(V) from aqueous solutions, Ind. Eng. Chem. Res. 48 (4) (2009) 2118–2124.

[14] P.R.S. Reddy, G. Agathian, A. Kumar, Ionizing radiation graft polymerized and modified flame retardant cotton fabric, Radiat. Phys. Chem. 72 (4) (2005) 511–516.

[15] T. Hirotsu, Plasma graft polymerization of glycidyl methacrylate and cyclodextrin immobilization, Thin Solid Films 506–507 (2006) 173–175.

[16] T. Kondo, H. Kubota, R. Katakai, Reactivity of glycidyl methacrylate grafted cellulose film prepared by grafting under ultrasonic irradiation, J. Appl. Polym. Sci. 74 (1999) 2462–2469.

[17] G. Torri, E. Vismara, A. Alberti, S. Bertini, G. Ciardelli, G. Gastaldi, Free-Radical Functionalized Polysaccarides (2003) EP 1 492 820, WO03078471.

[18] A. Alberti, S. Bertini, G. Gastaldi, N. Iannaccone, D. Macciantelli, G. Torri, E. Vismara, Electron beam Irradiated textile cellulose fibres. ESR studies and derivatisation with glycidyl methacrylate, Eur. Polym. J. 41 (2005) 1787–1797.

[19] G. Strukul (Ed.), Catalytic Oxidations with Hydrogen Peroxide as Oxidant, Kluwer Academic Publishers, Netherland, 1992.

[20] D.R. Lide (Ed.), CRC Handbook of Chemistry and Physics, 84th ed., CRC Press, 2004.

[21] N. Agmon, W. Rettig, C. Groyh, Electronic determinants of photoacidity in cyanonaphthols, J. Am. Chem. Soc. 124 (6) (2002) 1089–1096.

[22] G.H. Lu, J. Tang, X. Yan, Y.H. Zhao, Correlation for the structure and biodegradability of substituted benzenes in Songhua river water, Chem. J. Internet 3 (7) (2001) 34.

[23] J.H. Richards, S. Walker, Dipole moment and infrared studies of solvent effects on inramolecular hydrogen bonding. Part 2—Nitrophenols and nitronaphthols, Trans. Faraday Soc. 57 (1961) 406–411.

[24] B. Focher, M.T. Palma, M. Canetti, G. Torri, C. Cosentino, G. Gastaldi, Structural differences between non-wood plant celluloses: evidence from solid state NMR, vibrational spectroscopy and X-ray diffractometry, Ind. Crops Prod. 13 (2001) 193–208.

[25] S. Azizian, Kinetic models of sorption: a theoretical analysis, J. Colloid Interface Sci. 276 (2004) 47–52.

[26] F. Gimbert, N. Morin-Crini, F. Renault, P.M. Badot, G. Crini, Adsorption isotherm models for dye removal by cationized starch-based material in a single component system: error analysis, J. Hazard. Mater. 157 (2008) 34–46.

[27] R. Niwas, U. Gupta, A.A. Khan, K.G. Varshney, The adsorption of phosphamidon on the surface of styrene supported zirconium (IV) tungstophosphate: a thermodynamic study, Colloids Surfaces A: Physicochem. Eng. Aspects 164 (2000) 115–119.

[28] E. Tutem, R. Apak, C.F. Unal, Adsorptive removal of chlorophenols from water by bituminous shale, Water Res. 32 (1998) 2315–2324.

[29] O. Hamdaoui, E. Naffrechoux, Modeling of adsorption isotherms of phenol and chlorophenols onto granular activated carbon. Part I. Two-parameter models and equations allowing determination of thermodynamic parameters, J. Hazard. Mater. 147 (2007) 381–394.

[30] S.J. Allen, Q. Gan, R. Matthews, P.A. Johnson, Comparison of optimized isotherm models for basic dye adsorption by kudzu, Bioresour. Technol. 88 (2003) 143–152.

[31] Yuh-Shan Ho, Selection of optimum sorption isotherm, Carbon 42 (2004) 2115–2116.

[32] K.V. Kumar, Comparative analysis of linear and non-linear method of estimating the sorption isotherm parameters for malachite green onto activated carbon, J. Hazard. Mater. 136 (2006) 197–2002.

[33] K.V. Kumar, Optimum sorption isotherm by linear and non-linear methods for malachite green onto lemon peel, Dyes Pigments 74 (2007) 595–597.